Journal of Basic Physical Research ISSN: 2141-8403 Prints, 2141-8411 Online
Vol.14, Issue 2, October, 2025, pp. 61 – 78, Available online at https://journals.unizik.edu.ng/jbpr/

PREDICTING COAL QUALITY USING ELECTRICAL RESISTIVITY AND CHEMICAL TECHNIQUES FOR ENHANCED RESOURCE EVALUATION IN PARTS OF THE NORTHERN ANAMBRA BASIN, NIGERIA

[1]Oyubu, F., [1]Anakwuba, E. K., and [1]Chinwuko, A. I.
Department of Applied Geophysics, Nnamdi Azikiwe University Awka, Nigeria
Corresponding Author's Email: oyubufestus@gmail.com

Abstract
The purpose of the study was to correlate resistivity signatures with coal quality parameters for possible enhanced resource evaluation. The method used vertical electrical sounding (VES) and 2D electrical resistivity imaging (ERI) alongside coal samples, which were collected and subjected to chemical analysis to determine their percentage composition regarding proximate and ultimate analyses. The resistivity results, along with the borehole data, reveal five to nine lithological layers, including coal seams embedded within alternating sandstone and shale beds. Coal seam thickness ranges from 0.5 m to 6.1 m, with the thickest seams and mineable overburden observed in the western part of the study area. The geoelectric results also depict that the overburden thickness varies between 5 m and 140 m across the study area. A strong correlation was established between high resistivity values (>16,000 Ω-m) and high coal quality, characterized by low moisture (2.5-9.5%), low ash (2-16%), high fixed carbon (36-58%), and high calorific values (4400-6800 kcal/kg). The results depict that the lower resistivity zones were associated with lower-grade coal. The integrated results show that the study area possesses a total estimate of coal resources at 23.86 million metric tonnes, with an overall strip ratio of 22.63. The results show that low-sulfur zones (< 0.6) correspond to slightly high resistivity, implying minimal conductive sulfur-bearing compounds, while areas of higher sulfur (0.6-0.8%), higher oxygen content (11.4% - 14.4%), and higher ash content (16% - 34%) align with lower resistivity, highlighting zones requiring environmental monitoring. The study concludes that integrating electrical resistivity and coal sample analysis can serve as a reliable proxy for predicting coal quality and optimizing resource extraction strategies across the study area and the world at large.

Keywords*: 2D Electrical Resistivity Imaging (ERI), Coal seam, Proximate Analysis, Ultimate Analysis, and Sulfur Distribution*

Introduction

Coal remains a backbone of global energy supply, particularly for electricity generation, where it accounts for approximately 38% of global output and 27% of total energy consumption (https://www.iea.org/reports /coal 2018). It is primarily composed of carbon and contains variable proportions of hydrogen, sulfur, oxygen, nitrogen, and trace elements, including mineral matter (Onoduku, 2014). Due to its abundance, cost-effectiveness, and ease of transportation, coal continues to be a critical fuel for numerous industries, including iron, steel and cement production (Schnapp and Smith, 2012). Despite growing emphasis on renewable energy, coal persists as a dominant energy source, especially in developing nations (Coal Industry Advisory Board, 2008). In many countries, coal is the primary source of energy (Tutmez *et al*., 2013; Morrice and Colagiuri 2013; Saini *et al.*, 2016), and it plays a strategic role in achieving energy security and economic growth. Nations such as Poland, South Africa, China, and Australia rely on coal for over 90%, 92%, 77%, and 76% of their electricity needs, respectively (World Coal Institute, 2009). The global coal mining industry employs approximately 8 million people and generates annual revenues exceeding US$900 billion (Global Coal Mining Industry, 2019). In 2018, global coal demand increased by 1.4%, primarily driven by India and China, exceeding the average growth rate of the previous decade (BP, 2019). Projections indicate that coal will continue to be a major contributor to global energy demand in the coming decades (Qin *et al*., 2015).

However, the extensive use of coal has raised significant environmental and public health concerns. Activities related to coal storage, transportation, combustion and processing release harmful trace elements such as lead (Pb), mercury (Hg), fluorine (F), and arsenic (As) into the environment (Baruah and Khare, 2010; U.S. Environmental Protection Agency, 2005; Xiao *et al*., 2016). These contaminants necessitate effective mitigation strategies to reduce their environmental impact (Rajak *et al*., 2019; Singh *et al*., 2015). While international climate goals call for a swift reduction in coal use without carbon capture and storage technologies (Luderer *et al*., 2018), many developing economies still rely heavily on coal to meet industrial and energy demands (Kalkuhl *et al*., 2019). Beyond its conventional uses, coal is increasingly being explored as a secondary source for strategic and rare earth elements (REEs). The scarcity of REEs such as Al, As, Cr, Ni, Se, Ce, La, Ga, and Ge has led to research on extracting these elements from coal ash, a move that could offer environmentally sustainable alternatives to conventional mining (Mohammadi *et al*., 2015; Mayfield and Lewis, 2013).

In Nigeria, coal once played a pivotal role in powering key sectors such as railway transportation, cement production, and electricity generation. However, production has declined in recent decades (Odesola *et al*., 2013), worsening the country's energy crisis. Revitalizing the coal sector is essential for meeting Nigeria's growing energy demand. The country is endowed with substantial coal reserves, primarily located within the Anambra Basin (Carter *et al*., 1963; Obaje *et al*., 1994), comprising lignite, sub-bituminous, and bituminous coal. These deposits are suitable for diverse industrial applications, including boiler fuel, gas production, domestic heating and the manufacturing of chemicals, including waxes, resins, adhesives, and dyes (Ministry of Mines and Steel Development, 2010). Notable coal-bearing localities within the Anambra Basin include Ogboyoga and Okaba in Kogi State, Owukpa in Benue State, and the Enugu coalfields. These represent the most economically viable deposits (Fatoye and Gideon, 2013; Ojo, 2000), while smaller occurrences are found in Afikpo (Ebonyi State) and Koton-Karfi (Ehinola and Adene, 2008). The present study seeks to model and evaluate these coal resources using an integrated approach involving coal sample analysis, electrical resistivity surveys, and geostatistical techniques.

Among geophysical tools, **Vertical Electrical Sounding (VES)** has been extensively utilized in coal exploration due to its affordability and effectiveness in delineating subsurface layers. Nevertheless, VES is not without limitations. One prominent challenge is **layer suppression**, where thin coal seams are masked by overlying thick or conductive layers such as shale or sandstone with similar resistivity values. This suppression effect leads to poor resolution and hampers accurate seam delineation, especially in stratigraphically complex formations. Despite this inherent limitation, the present research successfully overcame the suppression issue through methodological refinements. By adopting **closer current electrode spacing** across all 43 VES stations in the study area, the resolution of shallow subsurface layers was significantly enhanced. This allowed for the clear detection and delineation of thin coal seams relative to the overburden, affirming the potential of VES when properly optimized as a reliable and cost-effective technique for coal exploration. The findings of this study offer new insights into how traditional geophysical methods can be adapted to resolve long-standing challenges in coal seam mapping.

However, exploration and development of Nigeria's coal deposits have been hampered by limited geological assessment and a lack of integrated geophysical and chemical data. Many awarded exploration blocks have yet to undergo thorough geological assessment. While geophysical methods (electrical resistivity) are effective in mapping coal seams, their relationship with chemical parameters (for example, ash content, fixed carbon, calorific value,

moisture content) are not well established in existing literature. Also, a major limitation in VES application is **layer suppression**, particularly when thin coal seams are overlain by thick overburden. This suppression effect results in poor resolution and inaccurate delineation of coal seams, which undermines the reliability of subsurface interpretation and coal resource estimation. In many coal-bearing formations, the similarity in resistivity between coal seams and surrounding lithologies, coupled with the thin nature of coal layers, results in under-detection or total omission in resistivity profiles. Consequently, coal seam delineation, mine planning, and resource estimation are undermined. This research seeks to address this critical gap by applying a refined VES technique with closer electrode spacing, supplemented by exploratory core drilling data and chemical analysis of coal core samples, to enhance the resolution and reliability of coal seam detection.

Location and Geologic setting of the Study Area

The study area lies within Latitudes 7° 41’ 20’’ to 7° 43’ 17.7’’ and Longitudes 7° 10’ 49.6’’ to 7° 12’ 14.6’’ in the Northern Anambra Sedimentary Basin, Southeastern Nigeria (Fig. 1). The area, approximately 9 km², is accessible via the Ankpa-Otukpa road, located 9 km from Otukpa town.

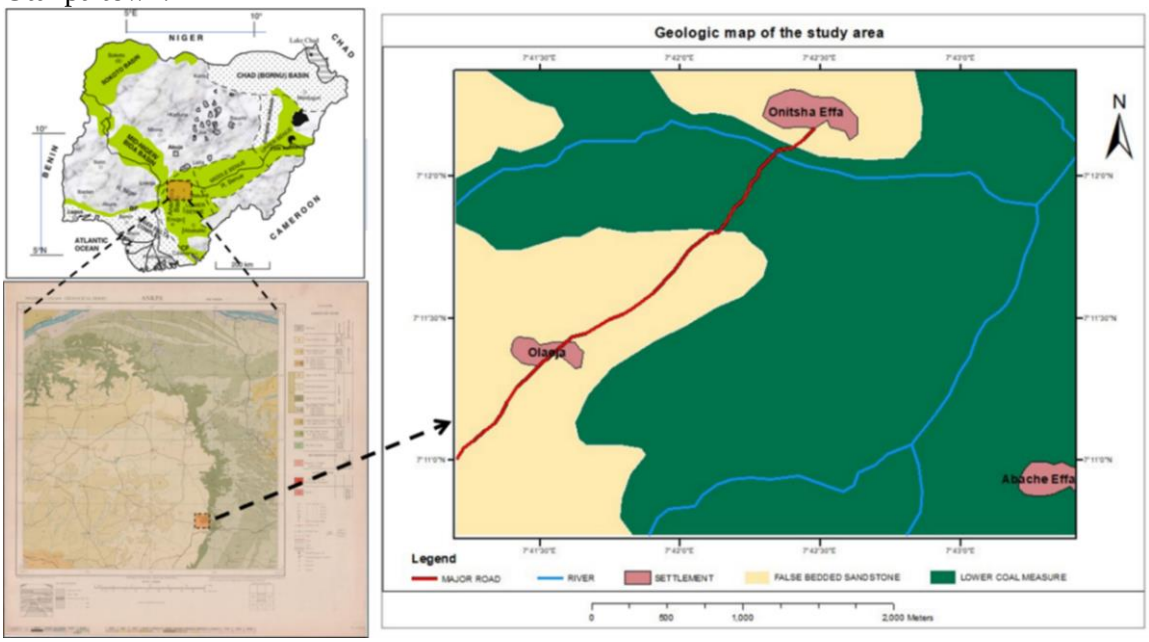


Fig. 1: (Geologic map of the study area.

The Anambra Basin’s sedimentary fill occurred between the Late Santonian and Danian, spanning approximately 11 million years (Nwajide, 2005). Gravity measurements estimate the basin’s sediment thickness to range from 1,000 to 4,500 m (Ladipo *et al*., 1992), with 3,000-3,500 m deposited during the Late Cretaceous (Late Campanian to Maastrichtian).The Campanian-Maastrichtian stratigraphic succession in the Anambra Basin includes; **Nkporo Shale Group (Campanian) which** consists of three Formations, namely; **Nkporo Shale (**composed of dark shales and mudstones interbedded with thin sandy shale and sandstone layers, (Kogbe, 1976); **Enugu Shale** (primarily composed of carbonaceous shales and coals, deposited in floodplain and swamp environments according Ladipo *et al*., 1992); **Owelli Sandstone (composed of the** major sand unit of the Enugu Shale, forming elongated, northeast-trending shoestring sand bodies that indicate fluvial/distributary channel deposition).

This is overlain by **Mamu Formation (Early to Late Maastrichtian)**, which according to Umeji (2002) contains three lithologic units: 1) **Lower Unit: which contains b**lack carbonaceous marine shales overlain by sandy shoreface deposits with heterolithic wave-rippled and flaser-bedded fine white sandstones interlaminated with dark grey mudstones; 2) **Middle unit:** Coal-bearing facies and 3) **Upper unit:** Fine to medium-grained sandstones with climbing ripple lamination. The studied section lies within the upper part of the coal-bearing facies.

Following this is the **Ajali Sandstone (Middle to Late Maastrichtian):** which is composed of thick, friable, poorly sorted sandstones, typically white but sometimes iron-stained (Reyment, 1965). Hence, the **Nsukka Formation (Late Maastrichtian to Danian)** conformably overlies the Ajali Sandstone. It consists of alternating sandstone, dark shale, and sandy shale with thin coal seams (Simpson, 1954). Thin limestone beds occur towards the top (Reyment, 1965).

Methodology

Vertical Electrical Sounding (VES)

Electrical resistivity surveying was carried out employing the vertical electrical sounding (VES) technique using Schlumberger electrode configuration at forty-three locations (Fig. 2) in east-west and north-south azimuth in the study area. VES point separation is between 400 m to 800 m such that the total area surveyed is approximately 9 km^2. A total of 43 VES were conducted with a minimum current electrode separation of 1.0 m and a maximum current electrode separation range of 300 - 400 m. The potential electrodes were made to remain fixed while the current electrodes spacing expands symmetrically about the centre of the spread. For large values of current electrode spacing the separation of the potential electrodes were also increase in order to maintain measurable potential at all times. To overcome the common suppression problem associated with VES, particularly in detecting thin coal seams beneath thick overburden, this study introduced a refined field approach. Closer and progressively adjusted current electrode spacing was adopted at all 43 VES locations. This modification significantly enhanced the vertical resolution of the shallow subsurface, enabling clearer differentiation between overburden layers and thin coal seams. As a result, this methodology improved the effectiveness of VES in mapping even relatively thin seams that would typically be suppressed. The measured ground resistance (R) at each VES point was converted into apparent resistivity (ρ_a) using the equation below.

$$\rho_a = GR$$

Where: G= Geometric factor.

The apparent resistivity data computed were plotted against one half of the current electrodes spacing (AB/2) on a bi-logarithmic graph and interpreted using an iterative computer software called WinResist software. The contrasts in electrical resistivity existing between lithological sequences in the subsurface (Lashkarripour, 2003) were used in the delineation of geoelectric layers. The resistivity and depths values obtained were used to produce geologic section in the study area.

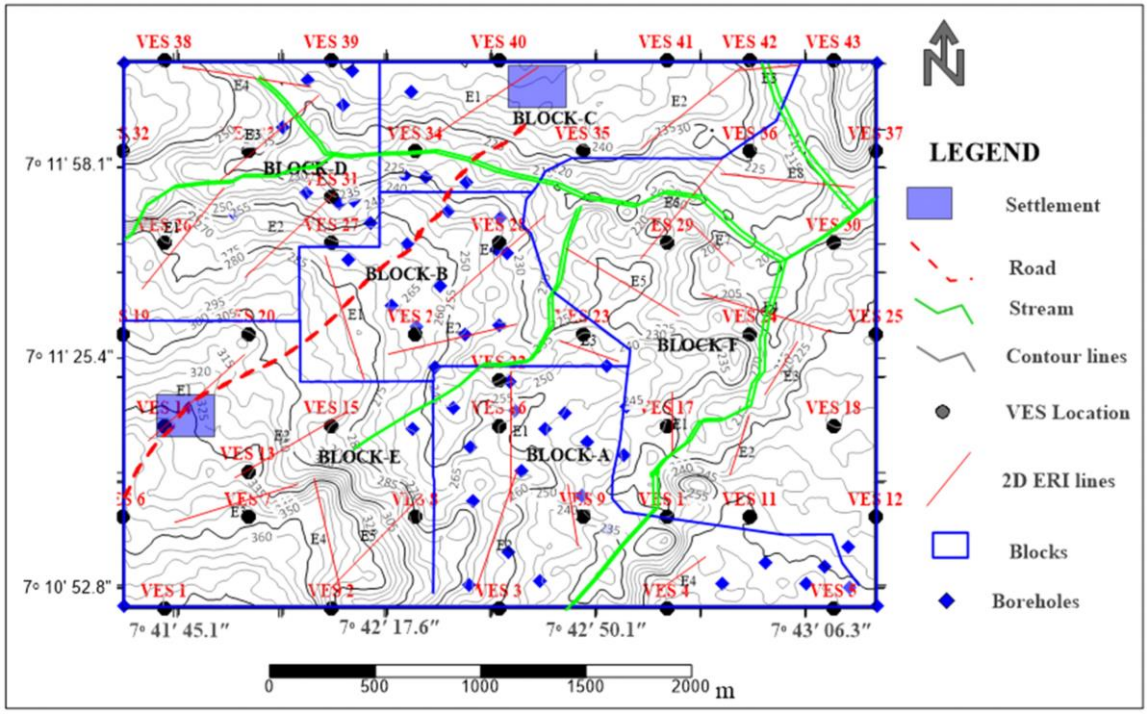


Fig. 2: Data acquisition map of the study area.

2D Electrical Resistivity Imaging (2D ERI)

A total of twenty-eight 2D ERI were conducted using dipole-dipole array. To ensure systematic spatial coverage Fig. 2 shows the locations of the 2D ERI profile lines.The study area was subdivided into six blocks (A- F), with the delineation informed by the spatial distribution existing **VES and borehole data**, which provided a clear understanding of **coal seam thickness, overburden variability**, and **non-coal-bearing zones** within the area. A resistivity meter called ABEM Tarameter L S (multielectrode imaging unit), with 64 electrodes connected to the resistivity meter through a multi-core reversible cable was used in the study. The survey objective was defined and the appropriate electrode array (dipole-dipole) was selected. The electrodes are laid out in straight lines and cables connected to the instrument such that the minimum traverse length was 315m for a 5m electrode intervals and maximum 630m for a 10 m electrode interval. The survey setting was configured and the automated data acquisition were done in all locations and saved. The measured apparent resistivity data were then downloaded from the equipment for further processing. The downloaded field data were processed, filtered, and inverted using the EarthImager software to generate 2D resistivity distributions and inverse model images of the subsurface. Topography correction was applied to each of the 2D profile lines to ensure accurate migration of subsurface features to their true positions. Inversion was carried out by comparing the measured apparent resistivity values with a calculated model to produce inverted 2D resistivity sections. These sections are presented in color-coded formats showing the lateral and vertical subsurface resistivity distribution. The vertical scale represents the investigation depth, while the lateral scale corresponds to horizontal ground distance. The resistivity range of each color is presented as a logarithmic color scale bar. The resulting resistivity images were used to characterize subsurface features and delineate the coal deposits and water-bearing zones in the area. High-resolution pseudosections with dense sampling at depths exceeding 100 meters were obtained efficiently.

2D Modeling of the Coal deposits

The final layering parameters obtained were used together with DGPS coordinates of the VES points and 2D ERI profile lines to construct an overburden thickness and resistivity map using Autocad and surfer softwares. Geoelectric sections tied to borehole data were also constructed along each traverse to obtain 2D stratigraphic models.

Borehole Core Data and Laboratory Measurement

Borehole coal core data were used as a control for apparent resistivity data intervals. Coal core samples were collected and subjected to chemical analysis to determine their percentage composition. This included Proximate Analysis on an Air-Dried Basis (ADB), which assessed % inherent moisture, % volatile matter, % ash, % fixed carbon and gross calorific value (Kcal/kg) to evaluate the quality of the coal for power-energy generation. Ultimate Analysis, an essential aspect of the coal characterization, quantified the elemental composition of organic material in the coal, including Carbon (C), Nitrogen (N), Hydrogen (H), Sulphur (S), and Oxygen (O).

Specific Gravity and Estimation of Coal Reserve

In this study, the specific gravity of coal was used as a conversion factor to estimate the tonnage of coal from the calculated volumes. Specific gravity is defined as the ratio of the density of coal to the density of water (1000 kg/m³ at 4°C). The specific gravity values used were obtained from laboratory analysis of coal core samples retrieved during drilling.

The coal reserve estimation for the study area was computed using the formula:

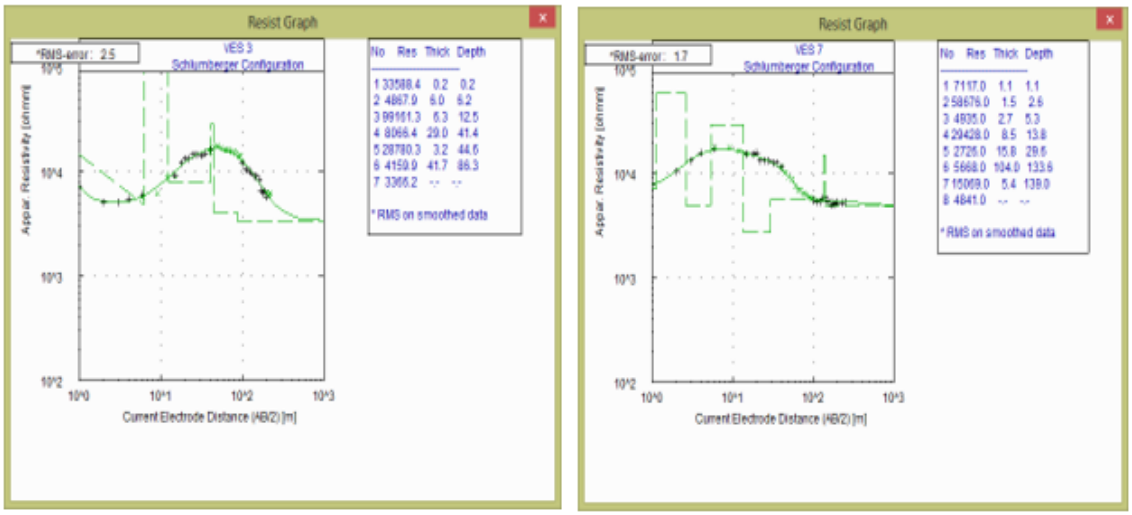
Coal Reserve (tonnes) = Area x Thickness x Specific Gravity

Where:

- Area is the surface area of the block (in square meters),
- Thickness is the average coal seam thickness (in meters), and
- Specific Gravity is dimensionless and based on lab results (1.2).

Results and Discussion

The qualitative interpretation of computer-generated model data curves reveals the presence of five to nine geoelectric layers. Some of the modeled curves are presented in Fig. 3.



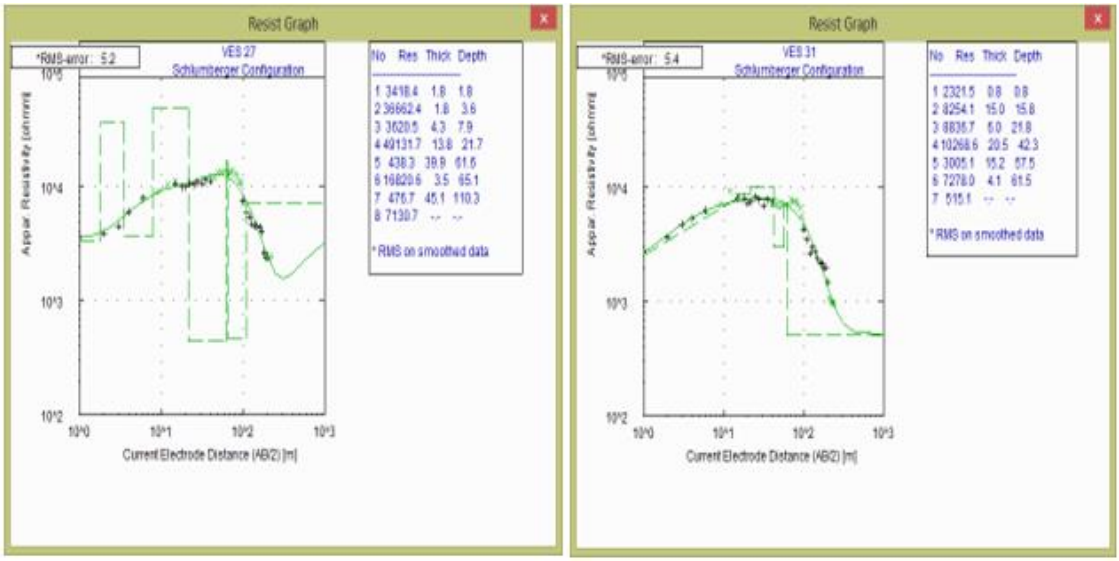


Fig. 3: Computer generated model data curves for VES 3, 7, 27 and 31

Geoelectric Sections and Stratigraphic Models

Geologic sections were generated based on interpreted layer resistivity values, layer thickness, and inferred lithology of the study area. Figure 4a-b illustrates the correlation between two VES points (VES-3 and VES-31) and two boreholes (OTA232 and OTA82), serving as ground truth for validating the interpretation of other data within the study area. Geologic sections (Fig. 5a-b) indicate the presence of five to nine geologic layers composed of sandy soil, sand, clay, clay-shale, shale, sandstone, coal, sandy shale / shaly sandstone, interbedded shale and sandstone.

Selected results of the 2D ERI resistivity inversion in the study area are presented in Fig 6a-c. The inverted resistivity model displays a variation in resistivity distribution, with high and low resistivity zones ranging from 1.0 to 100,000 Ω-m. Low resistivity zones (1.0-316 Ω-m), represented by deep blue to blue-green coloration, indicate groundwater saturation at depths. High resistivity zones (48,690-100,000 Ω-m), represented by red coloration, signify dry sand, compacted sandstone/shale. The ERI profiles were particularly effective in delineating **shallow and intermediate water-bearing zones**, helping to complement the VES results and to improve the overall understanding of hydrogeological conditions in the study area. This hydrological insight is essential for assessing mining feasibility, dewatering needs, and environmental impact. The shapes of the saturated zones suggest upward and lateral migration of groundwater in the study area. In most cases, the coal layer intersects the saturated zones along the profiles. To accurately reflect subsurface conditions, the placements of the coal seams in the inverted 2D ERI sections were guided by the integration of ground-truth data from VES and boreholes. Thus, the interpreted coal seam shown in the 2D ERI sections represents a geologically constrained model validated by the VES and borehole data of the study area.

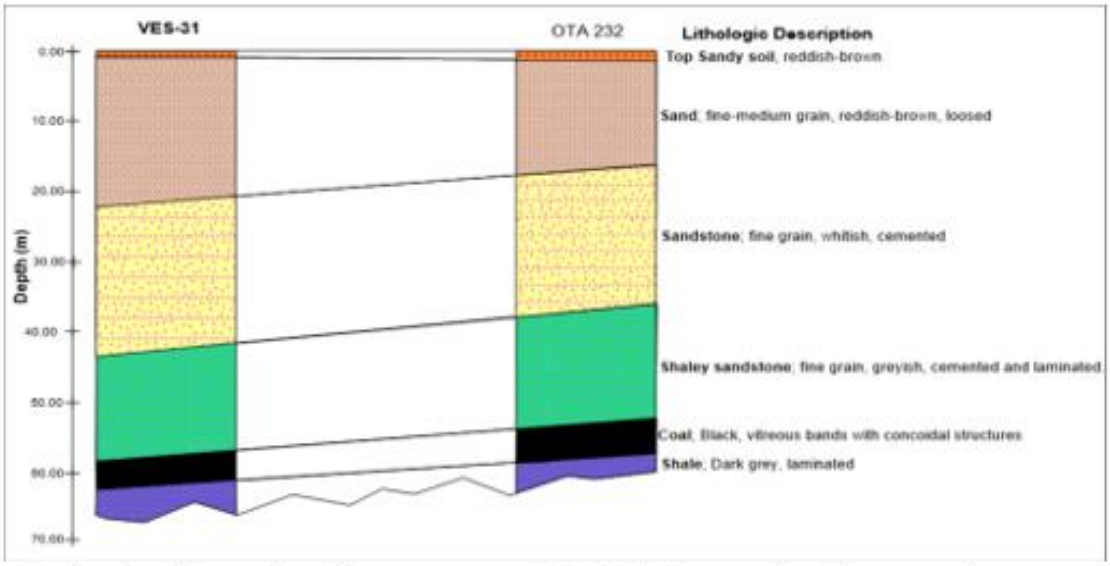


Fig. 4a: Correlation of geoelectric section with borehole for ground truthing at northern part of the study area.

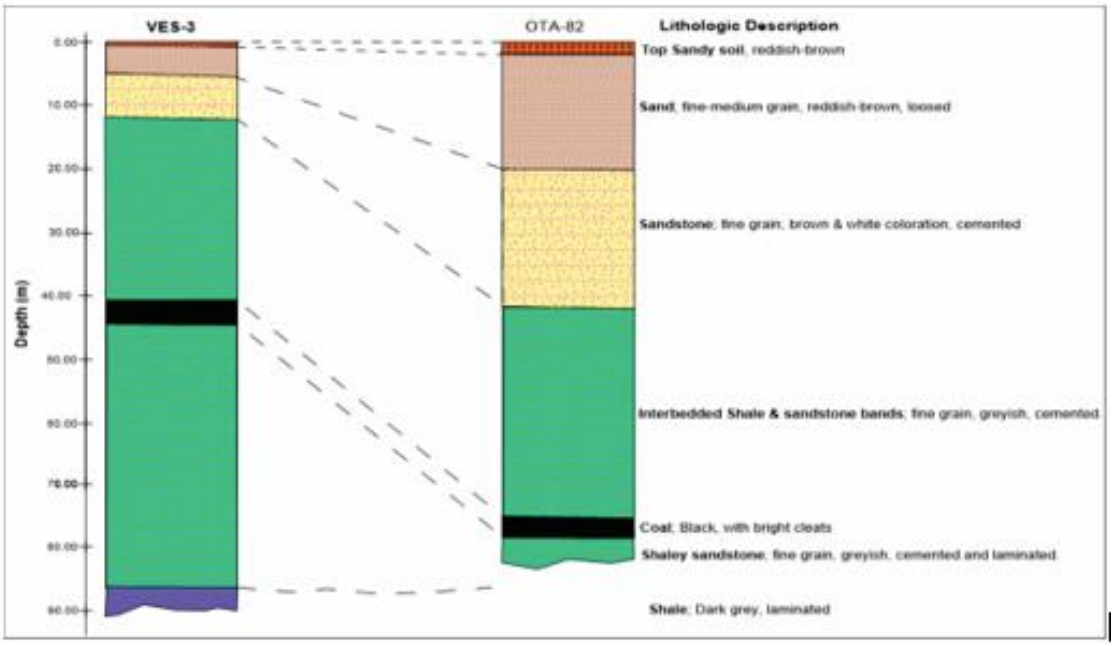
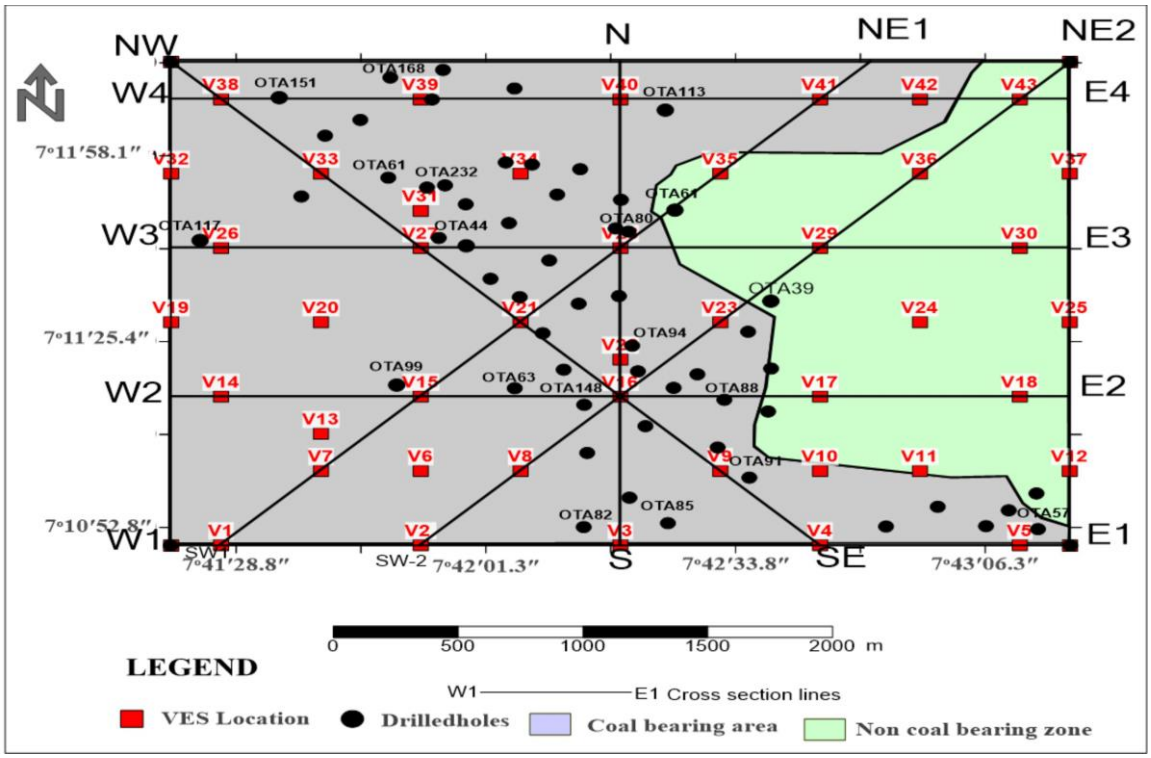


Fig.4b: Correlation of geoelectric section with borehole for ground truthing at southern part of the study area.



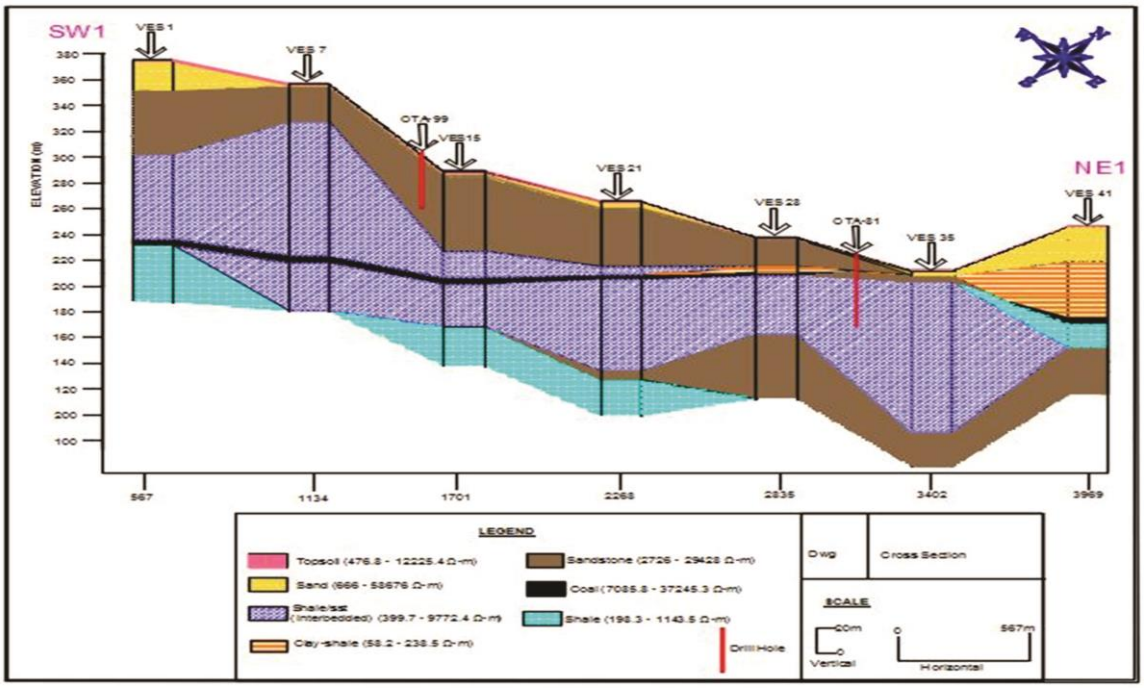


Fig.5a: Map showing VES points, boreholes and Geologic section along SW_1-NE_1 traverse.

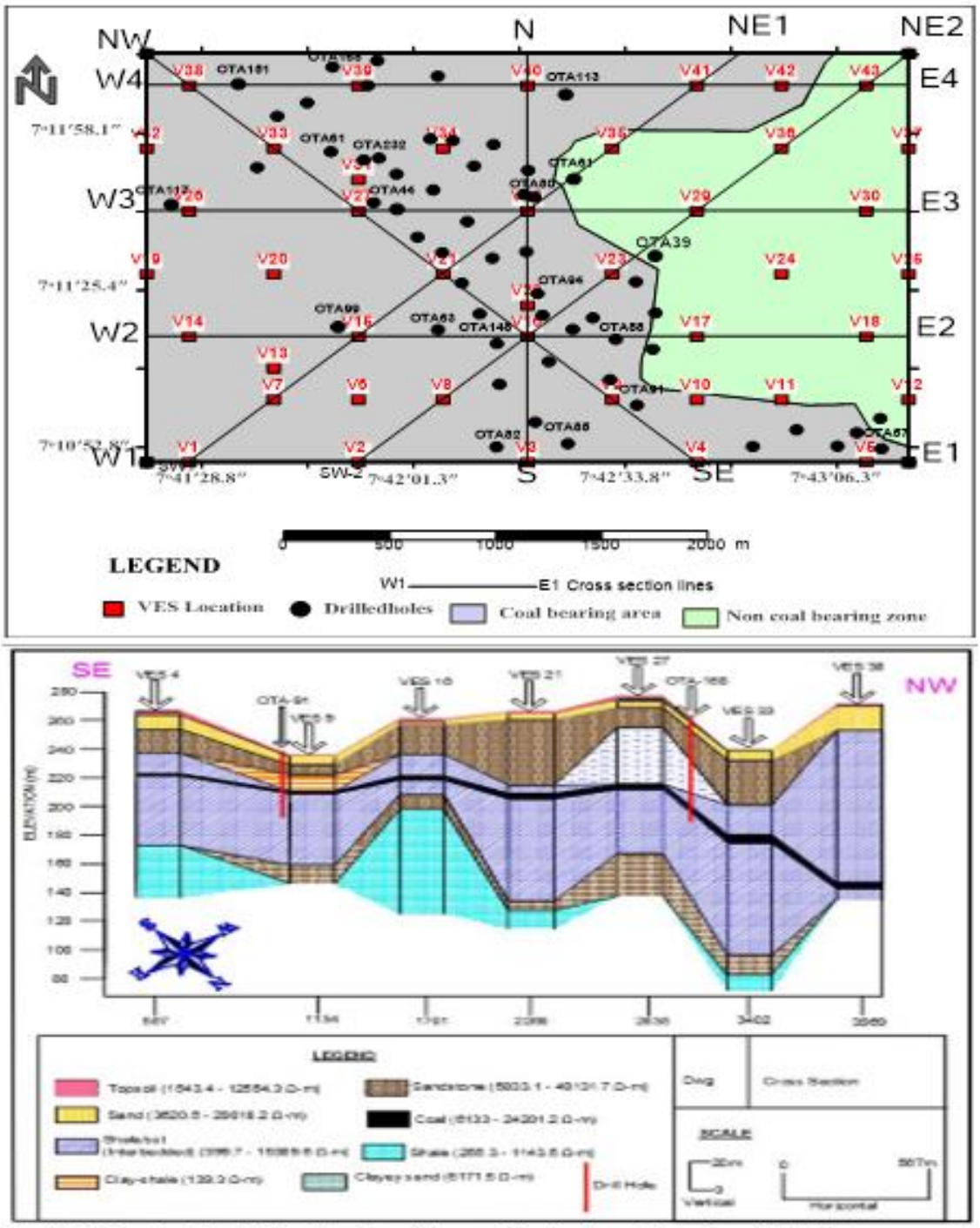


Fig. 5b: Map showing VES points, boreholes and Geologic section along SE-NW traverse.

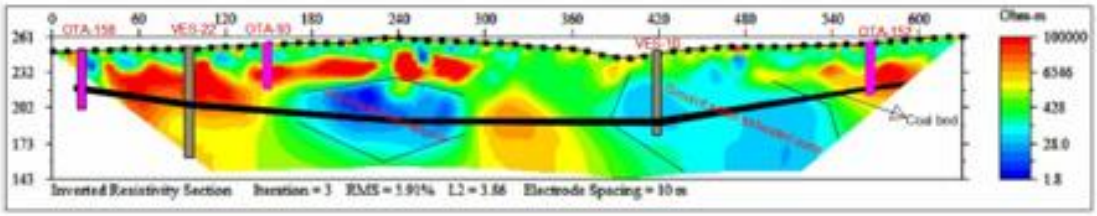


Fig. 6a: 2D resistivity structure and pseudosection for profile 1 (in Block A)

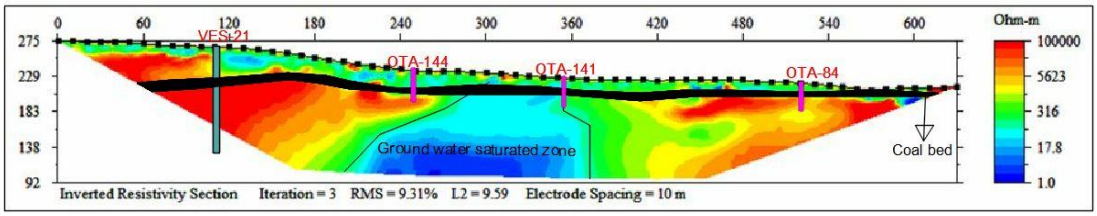


Fig. 6b: 2D resistivity structure and pseudosection for profile 2 (in Block B)

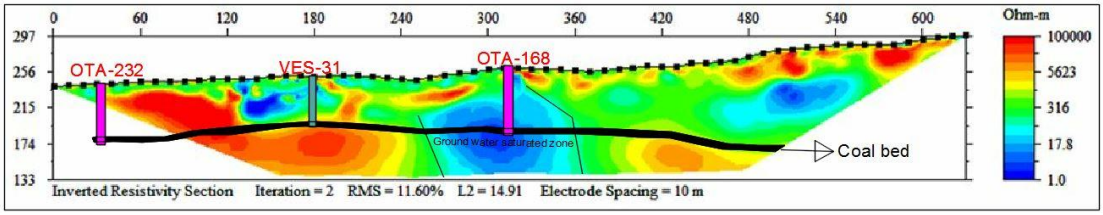


Fig. 6c: 2D resistivity structure and pseudosection for profile 2 (in Block D)

Overburden to Coal Thickness Relationship and Resource Estimation

The integration of overburden and coal seam thickness contour maps (Fig. 7a-b) reveals spatial trends critical to evaluating mining feasibility. In the central-eastern zone, thick coal seams exceeding 3.5 m are overlain by relatively thin overburden (15-30 m), indicating highly prospective areas for open-pit mining due to favorable stripping ratios and reduced operational costs. In contrast, the southwestern and northwestern zones, while hosting appreciable seam thicknesses (up to 5 m), are characterized by overburden depths exceeding 50 m. These conditions reduce the viability of surface mining but may support underground mining methods.

The surveyed coal-bearing area spans approximately 6,661,274 m². Using an average specific gravity of 1.2 and the calculated coal seam volume, the total estimated in-situ coal resource amounts to approximately 23.86 million metric tonnes. The computed average strip ratio across the study area is 22.63, reflecting the balance between overburden removal and coal recovery.

Table 1 presents the estimated coal resources, corresponding overburden volumes, and calculated strip ratios, while Table 2 details the spatial distribution of overburden thickness, associated coverage, and mean seam thickness across different zones.

These results offer critical input for resource classification, mining method selection, and economic viability assessments. The delineation of low-stripping zones with substantial seam thickness provides a strategic foundation for preliminary mine planning and development prioritization.

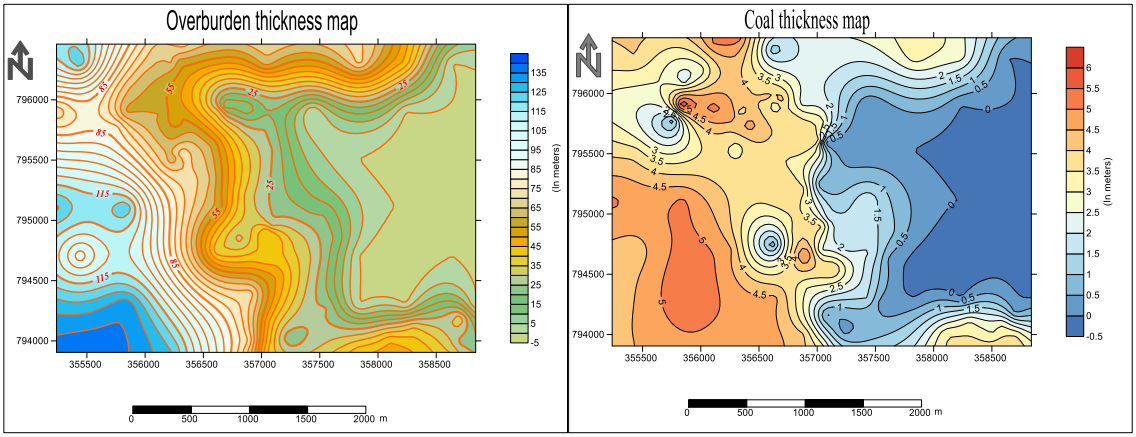


Fig. 7a: Overburden versus Coal thickness map

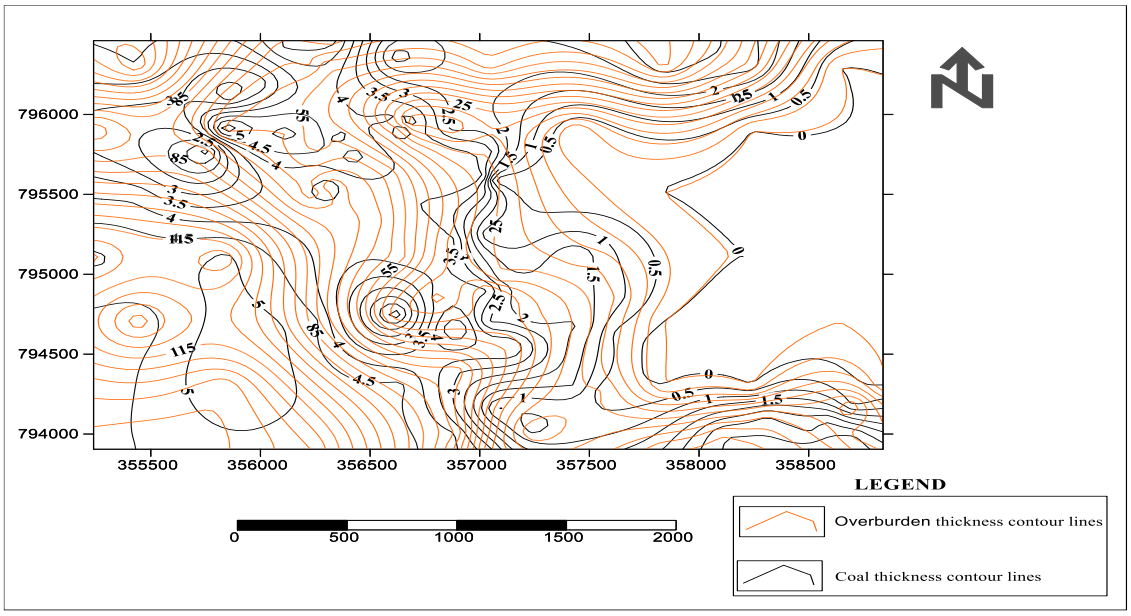


Fig.7b: Overburden versus coal thickness contour map overlaid

Table 1: Coal Resource Estimation and Overburden Analysis

BLOCK	Average Overburden Thickness (m)	Area (sq.m)	Av. Coal thickness (m)	Specific gravity	Resource in MT	Volume of Coal Seam (m^3)	Volume of Overburden (m^3)	Strip Ratio
A	36	1375472.0	2.5	1.2	4126415.88	3438679.90	49516990.56	14.40
B	36	1033110.3	2.25	1.2	2789397.92	2324498.27	37191972.24	16.00
C	37	1045397.2	2.25	1.2	2822572.33	2352143.61	38679694.92	16.44
D	90	1416006.4	3.25	1.2	5522425.04	4602020.87	127440577.80	27.69
E	110	1791288.4	4	1.2	8598184.22	7165153.52	197041721.80	27.50
TOTAL		**6661274.0**			**23858995.39**	**19882496.16**	**449870957.32**	**22.63**

Table 2: Coal overburden contour control

Overburden range (m)	Area (sq.m)	Av. Coal thickness (m)
5-25	1310340.66	2.50
25-55	1894081.85	3.00
55-80	1292896.59	4.00
80-140	2163955.16	4.25
TOTAL	**6661274.26**	

Relationship between Resistivity and Coal Quality Variation

Comparative analysis of the geophysical resistivity map and coal quality distribution maps (derived from proximate and ultimate analyses) reveals a strong spatial correlation between resistivity anomalies and coal characteristics in the study area (Fig. 8a-e). The resistivity anomalies align with significant variations in coal properties, establishing a reliable basis for coal quality prediction.

High resistivity zones (≥16,000 Ω·m), predominantly situated in the southwestern to northwestern parts of the study area, are indicative of coal seams with high grade attributes, including:

i. Lower moisture content (2.5% - 9.5%)
ii. Higher fixed carbon (36% - 58%)
iii. Higher gross calorific value (4400 – 6800 kcal/kg)
iv. Elevated carbon content (60% - 84%)
v. Higher hydrogen content (4.6% - 5.7%)

Conversely, low resistivity areas (<16,000 Ω·m), primarily located in the central and eastern sectors, correspond to coal seams with **higher moisture content (9.5% - 17.0%), lower fixed carbon, increased ash content (16% - 34%)** and higher oxygen content (11.4% - 14.4%) indicating lower-grade coal. These trends affirm that resistivity values are sensitive to coal composition and can be effectively employed as a non-invasive proxy for assessing coal quality in unexplored regions.

Spatial analysis also shows that the thickest coal seams are concentrated in the southwestern quadrant of the study area-coinciding with zones of high resistivity and enhanced fixed carbon values-suggesting economically attractive deposits. In contrast, thinner seams in lower resistivity zones exhibit diminished quality, characterized by elevated moisture and ash contents.

Environmental Considerations: Sulfur distribution across the basin is generally low, with concentrations ranging from 0.3% to 0.6% in northern and central pockets-areas that also exhibit relatively high resistivity, implying minimal conductive sulfur-bearing compounds. However, localized elevations in sulfur content (0.6% – 0.8%) are typically associated with low resistivity zones and warrant environmental monitoring to mitigate risks such as acid mine drainage.

Furthermore, oxygen-rich zones with elevated ash content may be prone to spontaneous combustion due to enhanced coal oxidation. These areas require vigilant stockpile

management, ventilation control, and fire prevention protocols to ensure operational and environmental safety.

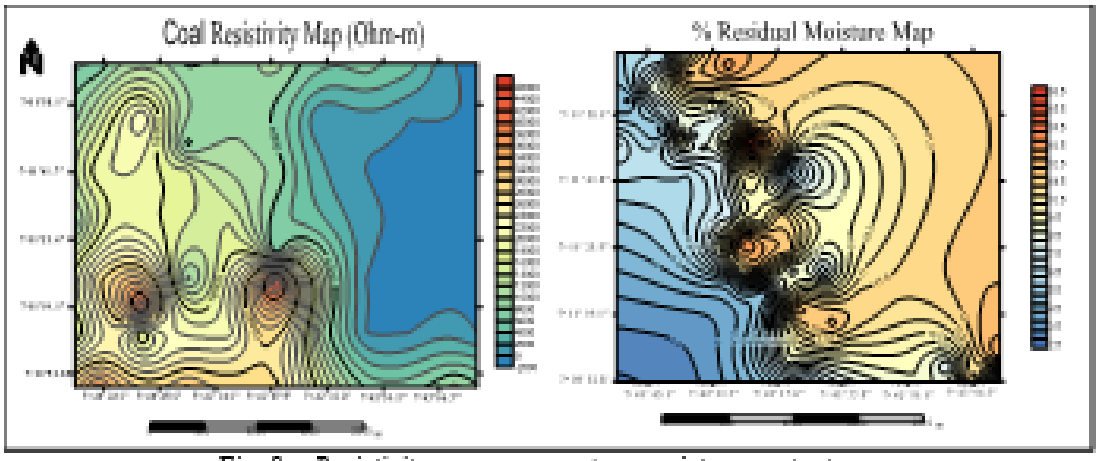


Fig. 8a: Resistivity versus percentage moisture content map

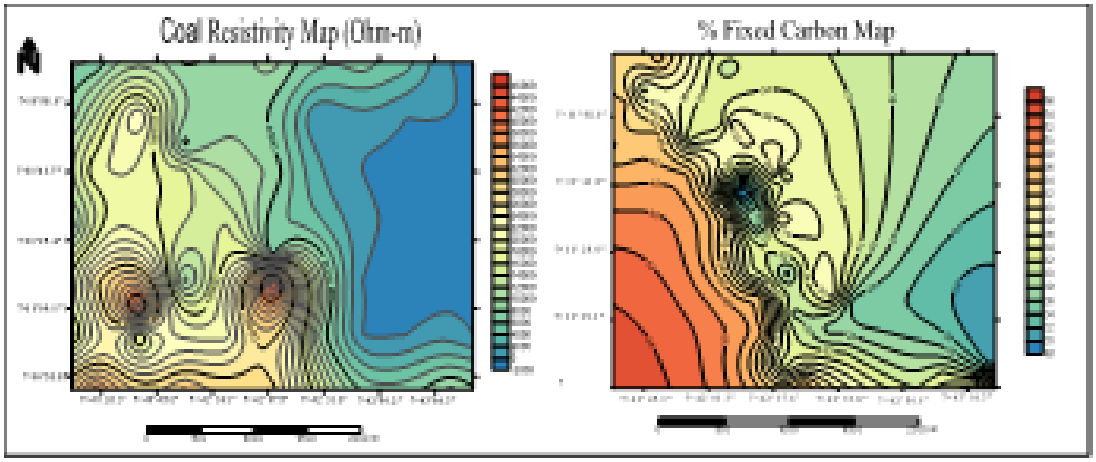


Fig.8b: Resistivity versus percentage fixed carbon map

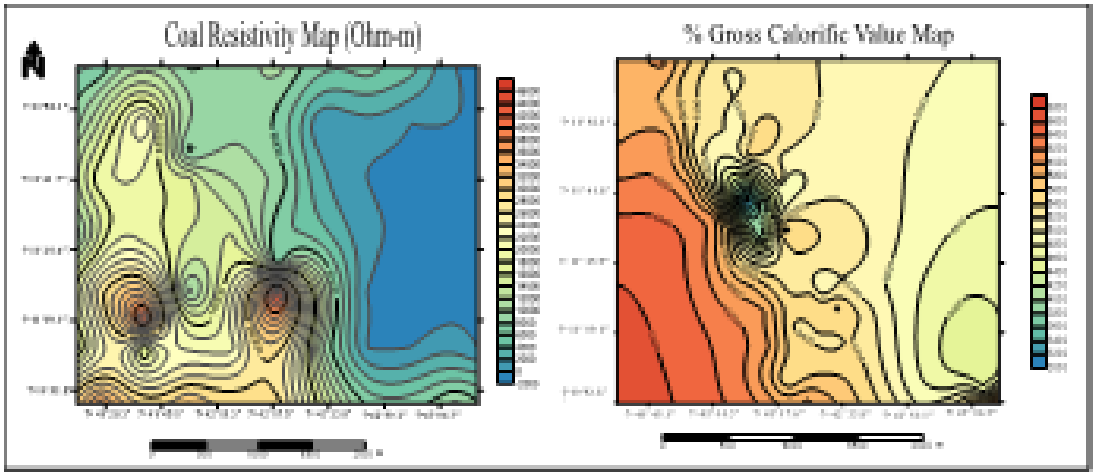


Fig.8c : Resistivity versus gross calorific value (GCV) map

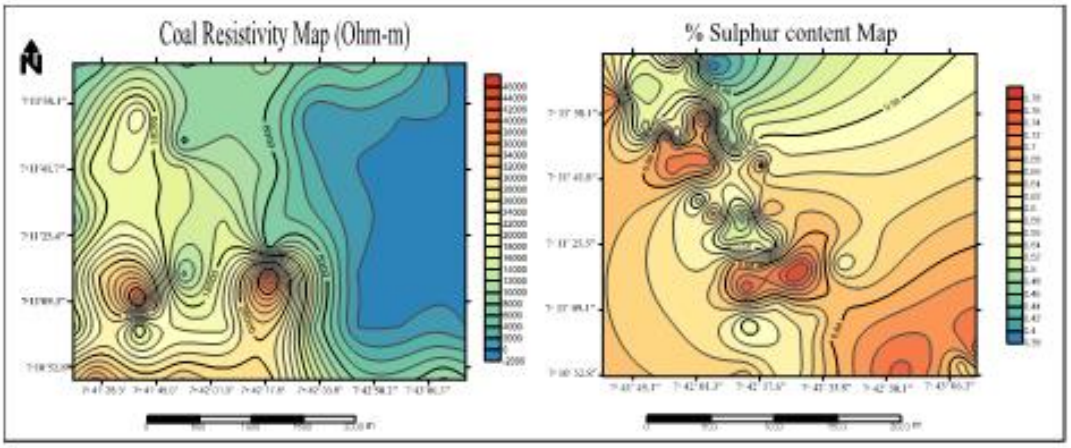


Fig.8d: Resistivity versus percentage sulphur content map

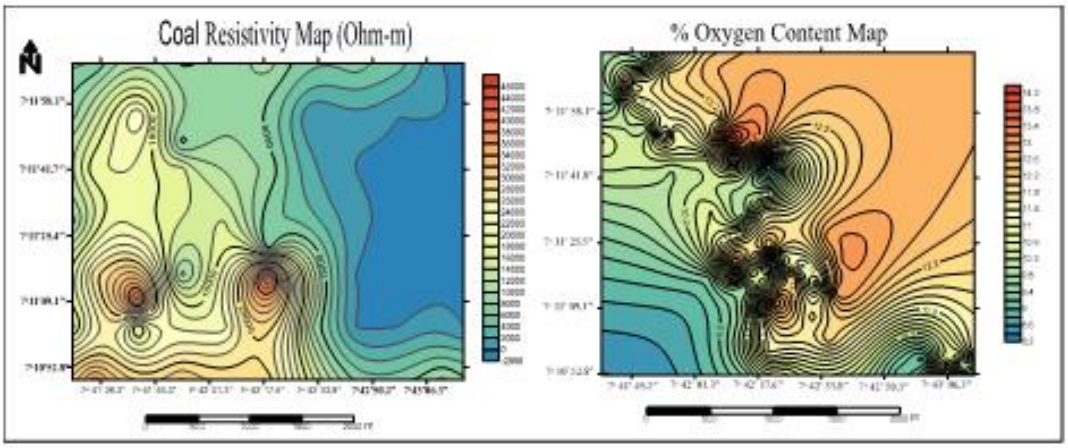


Fig. 8e: Resistivity versus percentage oxygen content map

Conclusion

This study demonstrates the effectiveness of integrating geophysical (electrical resistivity) and chemical (proximate and ultimate) methods in delineating coal seams and evaluating coal quality in the northern Anambra Basin, Nigeria. The integration yields a comprehensive framework for resource estimation, quality assessment, and extraction planning. Resistivity measurements revealed coal seams embedded within alternating sandstone and shale beds with values ranging from 4,854.1 to 46,615.8 Ω·m, a range influenced by moisture, compaction, and mineral impurities. High resistivity zones (≥16,000 Ω·m) are closely associated with high quality coal characterized by low moisture (2.5% - 9.5%), high fixed carbon (36% - 58%), low ash (2% - 16%), and elevated calorific values (4400 - 6800 kcal/kg). These zones, primarily located in the western part of the study area, represent the most viable targets for economic exploitation due to moderate and mineable overburden depth, and seam thicknesses (up to 6.1 m).

In contrast, central and eastern areas, defined by lower resistivity (<16,000 Ω·m), exhibit coal seams with higher moisture and ash contents, reduced calorific values (3000 - 4400 kcal/kg), and thinner seam development, thereby representing lower-grade deposits with reduced economic potential. The study estimated a total coal resource of approximately 23.86 million metric tonnes with an average strip ratio of 22.63. In addition, 2D resistivity models effectively visualize subsurface coal geometry, overburden distribution, and hydrogeological influences.

From an environmental perspective, sulfur levels are generally low (0.3% - 0.6%), reducing potential for acid mine drainage in most parts of the region. However, localized zones with elevated sulfur content (0.6% – 0.8%) and high oxygen levels require monitoring and targeted mitigation strategies, including dewatering and combustion protective measures.

References

Baruah, B. P., & Khare, P. (2010). Mobility of trace and potentially harmful elements in the environment from high sulfur Indian coal mines. *Applied Geochemistry, 25*, 1621–1631. https://doi.org/10.1016/j.apgeochem.2010.08.004

BP (2019). Full report – BP Statistical Review of World Energy 2019. London: BP, p.1.c.

Coal Industry Advisory Board (CIAB). (2008). *Clean coal technologies: Accelerating commercial and policy drivers for deployment*. International Energy Agency, Paris.

Carter, J. D., Barber, W., Tait, E. A., & Jones, G. P. (1963). *The geology of parts of Adamawa, Bauchi and Borno provinces in northeastern Nigeria*. Geological Survey of Nigeria Bulletin No. 30:108.

Ehinola, O. A., & Adene, T. M., (2008). Preliminary Investigation on Acid Generating Potential of Coals from Benue Trough, Nigeria. Petroleum and Coal 50(3), 19-26.

Fatoye, F. B., & Gideon, Y. B. (2013). Geology and occurrences of limestone and marble in Nigeria. *Journal of Natural Sciences Research, 3*(11). https://www.iiste.org

Global Coal Mining Industry (2019). Market Research Report (ibisworld, 2019); https://www.ibisworld.com/global/market-research-reports/global-coal-mining-industry/https://www.iea.org/reports /coal 2018

Kalkuhl, M., Steckel, J. C., Montrone, L., Jacob, M., Peters, J., & Edenhofer, O. (2019). Successful coal phase-out requires new models of development. *Nature Energy, 4*, 897–900. https://doi.org/10.1038/s41560-019-0456-5

Kogbe, K. C. (1976). Paleogeographic history of Nigeria from the Albian times. In C. A. Kogbe (Ed.), *Geology of Nigeria* (2nd ed., pp. 15–35). Elizabethan Publishing Co.

Ladipo, K. O., Nwajide, C. S., & Akande, S. O. (1992). Cretaceous and Paleogene sequences in the Abakaliki and Anambra basins, southeastern Nigeria. *National Symposium on Geology of Deltas*.

Lashkarripour, G. R. (2003). An investigation of groundwater condition by geoelectrical resistivity method: A case study in Korin aquifer, southeastern Iran. *Journal of Spatial Hydrology, 3*(1), 1–5.

Luderer, G., Vrontisi, V., Bertram, C., Edelenbosch, O. Y., Pietzcker, R. C., Rogelj, J., Deboer, H.S., Drouet, L., Emmerling, J., Fricko, O., Fujimori, S., Havlik, P., Iyer, G., Keramidas, K., Kitous, A., Pehl, M., Krey, V., Riahi, K., Saveyn, B., Tavoni, M.,

Vuuren, D.P.V., & Kriegler, E. (2018). Residual fossil CO_2 emissions in 1.5–2 °C pathways. *Nature Climate Change, 8*, 626–633. https://doi.org/10.1038/s41558-018-0198-6

Mayfield, D.B., & Lewis, A.S., (2013). Environmental review of coal ash as a resource for rare earth and strategic elements. World of coal Ash (WOCA) conference, Lexington KY. April 22-25. Available: http://www.flyash.info/2013/051-mayfield-2013.pdf

Ministry of Mines and Steel Development, Nigeria. (2010). *Coal resource information*. http://www.mmsd.gov.ng/Downloads/coal.pdf

Mohammadi, M., Forsberg, K., Kloo, L., Martinez, delacruz, J., Rasmuson, Å., (2015). Separation of ND(III), DY(III) and Y(III) by solvent extraction using D2EHPA and EHEHPA. Hydrometallurgy 2015(0). Available: http:// www.sciencedirect.com/ science/article/pii/S 0304386X15300116

Morrice, M., & Colagiuri, R. (2013). Coal mining, social injustice and health: A universal conflict of power and priority. *Health & Place, 19*, 74–79. https://doi.org/10.1016/j.healthplace.2012.11.016

Nigerian Geological Survey Agency (NGSA). (1957). *Nigerian geological series: Ankpa Sheet 63* (1st ed.).

Obaje, N. G. (2009). *Geology and mineral resources of Nigeria* (1st ed.). Springer London. https://doi.org/10.1007/978-3-540-92685-6

Nwajide, C. S. (2005). Anambra Basin of Nigeria: Synoptic basin analysis as a basis for evaluating its hydrocarbon prospectivity. In C. O. Okogbue (Ed.), *Hydrocarbon potentials of the Anambra Basin* (pp. 1–46). Great AP Express Publishers Ltd.

Obaje, N. G. (1994). Coal petrography, microfossils and palaeoenvironments of Cretaceous coal measures in the Middle Benue Trough of Nigeria. *Tübinger Mikropaläontologische Mitteilungen, 11*, 1–165.

Odesola, I. F., Samuel, E., & Olugasa, T. (2013). Coal development in Nigeria: Prospects and challenges. *International Journal of Engineering and Applied Sciences, 4*(1). http://www.eaas-journal.org

Ojo, J. S. (2000). *Geophysics, energy resources and the environments*. An Inaugural Lecture delivered on the 7th of March at the Federal University of Technology, Akure, Nigeria.

Onoduku, U. S. (2014). Chemistry of Maiganga coal deposit, Upper Benue Trough, northeastern Nigeria. *Journal of Geosciences and Geomatics, 2*(3), 80–84.

Qin, S., Sun, Y., Li, Y., Wang, J., Zhao, C., and Gao, K., (2015). Coal deposits as promising alternative sources for gallium. Earth-science Reviews 150: 95–101.

Rajak, P. K., Singh, V. K., Singh, A. L., Kumar, N., Kumar, O. P., Singh, V., Kumar, A., Rai, A., Rai, S., Naik, A.S., & Singh, P. K. (2019). Study of minerals and selected environmentally sensitive elements in Kapurdi lignites of Barmer Basin, Rajasthan, western India: Implications to environment. *Geosciences Journal*, 1–18. https://doi.org/10.1007/s12303-019-0011-3

Reyment, R. A. (1965). *Aspects of the geology of Nigeria*. Ibadan University Press, 445.

Saini, V., Gupta, R. P., & Arora, M. K. (2016). Environmental impact studies in coalfields in India: A case study from Jharia coal-field. *Renewable and Sustainable Energy Reviews, 53*, 1222–1239. https://doi.org/10.1016/j.rser.2015.09.046

Schnapp, R., & Smith, J. (2012). *Coal information*. Paris, France: International Energy Agency.

Simpson, S. (1954). The Nigerian coalfields: The geology of parts of Onitsha, Owerri and Benue Province. *Geological Survey of Nigeria Bulletin, 24*, 49–50.

Singh, P. K., Rajak, P. K., Singh, M. P., Naik, A. S., Singh, V. K., Raju, S. V., & Ojha, S. (2015). Environmental geochemistry of selected elements in lignite from Barsingsar and Gurha mines of Rajasthan, western India. *Journal of the Geological Society of India, 86*, 23–32. https://doi.org/10.1007/s12594-015-0211-1

Tutmez, B., Hozatli, B., & Cengiz, A. K. (2013). An overview of Turkish lignite qualities by logistic analysis. *Journal of Coal Science & Engineering, 19*, 113–118. https://doi.org/10.1007/s12404-013-0105-5

U.S. Environmental Protection Agency. (2005). *Control of mercury emissions from coal-fired electric utility boilers: An update*. U.S. EPA.

Umeji, A. C. (2002). *Evolution of the Abakaliki and the Anambra sedimentary basins, southeastern Nigeria*. Shell Chair Project Report submitted to S.P.D.C. Nig. Ltd. 155pp.

World Coal Institute (2009). The coal resources: A comprehensive overview of coal (Research report). Retrieved from http://www. worldcoal.org

Xiao, L., Zhao, B., Duan, P., Shi, Z., Ma, J., & Lin, M. (2016). Geochemical characteristics of trace elements in the No. 6 coal seam from the Chuancaogedan Mine, Jungar Coalfield, Inner Mongolia, China. *Minerals, 6*(28). https://doi.org/10.3390/min6010028